

THERMO-ELASTIC STUDY OF SANDWICH PLATES BY ALTERNATIVE HIERARCHICAL FINITE ELEMENT METHOD BASED ON REDDY'S C1HSDT

S.M.N. Serdoun^{*1}, *S.M.Hamza Cherif*², *Omar Sebbane*³

^{*1} Laboratory of Computational Mechanics (MECACOMP), University of Tlemcen, B.P. 230,
Tlemcen 13000, Algeria

² Higher School of Applied Sciences, Department of Technology, University of Tlemcen, B.P. 230,
Tlemcen 13000, Algeria

³ Faculty of Engineering, Department of Mechanical Engineering, University of Tlemcen, B.P. 230,
Tlemcen 13000, Algeria

* Corresponding author; E-mail: serdounn2006@hotmail.com

Received: 11 May 2018; Accepted: 28 June 2018

The dynamic behavior of a structure is influenced by the environment in which it is located it among the community seeking more structure, we have the thermal loading, this work investigates a plate sandwich subjected to thermal stress, the modeling of the plate is made by a third order model developed by Reddy TSDT (Third Order Shear Deformation Theory), while the TLT theory (Theory Thermal Layers) is used to transform the three-dimensional problem to a two-dimensional thermal problem. Next, a rectangular-p element with four nodes at the vertices and four sides is used to model the structure, and the thermal conduction. In the structure part, the forms used functions are trigonometric family C0 type for membrane displacements and rotations and type C1 for inflected movements, the thermal portion is modeled by C0 types of shape functions where the degrees of freedom to the nodes are the temperature, the temperature gradient and the temperature curve, the thermoelastic study to determine the displacements of the submerged plate by the method of integration time PTIM (Precis Time Integration Method). Finally, a study of convergence of the developed numerical code is made, the found results are validated with those found in the literature, and different parametric studies are made for the sandwich plates in different situations, structure, and thermo- elastic.

Key words: *Free vibration, thick composites plates, sandwich plate, hierarchical finite element method, C1 HSDT, heat conduction, thermo-elastic analysis.*

I. Introduction

The theory of thermoelasticity represents a generalization of both the theory of elasticity and the theory of heat conduction in solids. It is a branch of applied mechanics that is concerned with the effects of heat on the deformation and stresses of solid bodies, which are considered to be elastic.

The simplifying assumptions made in CPT and FSDT are reflected by the high percentage errors in the results of thick plates analysis. For these plates, higher-order shear deformation theories (HSDT) are required. The HSDT ensure a zero shear-stress condition on the top and bottom surfaces of the plate, and do not require a shear correction factor, which is a major feature of these theories.

Nelson and Lorch [1], Lo et al. [2] presented a HSDT for laminated plates however the displacement field does not satisfy the shear-stress free condition on the top and bottom surfaces of the plate. Nayak et al. [3,4] investigate the free vibration and transient response of composite sandwich plates by using two C1 assumed strain finite element based on Reddy's third-order theory. Batra et al. [5] used a HSDT and the finite element method to analyse free vibrations and stress distribution in thick isotropic plate. Ambartsumian [6] proposed a higher-order transverse shear stress function to explain plate deformation. Soldatos and Timarci [7] suggested a similar approach for dynamic analysis of laminated plates. Various different functions were proposed by Reddy [8].

The problem of heat conduction is studied by solving the Fourier heat conduction equation. For temperature variations in composites, this has been the subject of several studies. Padovan [9] proposed a discretization with three-dimensional elements. The effort can be reduced by modeling a couple of layers with only a three-dimensional element Tamma et Yurko [10]. Where also to use a two-dimensional element with hierarchical form functions (version-p) Bose and Surana [11]. Rolfes [12] used the finite element method to solve the problem of temperature distribution in stratified plates, some studies have considered sandwich and multilayer plates with different materials, such as Heemskerk [13], where he studied the conductivity of sandwich plates for structures used in space, or also Novack [14] who used a new method for hybrid plates, the solution is given for the case of hulls as it is proposed by Brischetto [15], the geometry of the plate can be considered as a special case of the geometry of the shell when the radii of curvature are infinite. Brischetto and Carrera (Brischetto et Carrera, 2011) have proposed to solve the Fourier heat conduction equation in the case of orthotropic multilayer structures in order to obtain a temperature profile calculated in the direction of the thickness. The temperature profile is calculated for the thickness of two types of geometries, plates and shells.

The theory of thermoelasticity is considered an extension of the classical theory of isothermal elasticity, to those processes in which deformations and stresses are produced not only by mechanical forces, but also by temperature variations. Bending of composite and laminate laminates or sandwich shell was evaluated by means of a linear temperature profile across the thickness direction by Khare et al [17]. Khdeir [18] solved thermoelastic governing equations by assuming a linear or constant temperature profile across the thickness. An interesting process to analyze the thermal stresses in hulls, as there is Birsan [19] for two given temperature fields. Other computer models have used a calculated temperature profile, because in the case of multilayer anisotropic structures, because in the case of multilayer anisotropic structures, the temperature profile is never linear, even when the plate or shell is thin, an incorrect temperature profile gives an erroneous thermal load which leads to larger errors, even if the model is structurally accurate Carrera [20, 21]. A finished shell element was developed by Rolfes et al [22]. they analyzed composite structures simultaneously loaded by mechanical and thermal loads, the temperature profile was assumed linear or quadratic in the direction of the thickness, then introduced

into the conduction equation of the Fourier heat. The conduction equation of the Fourier heat has been solved by the authors for multilayer composite hulls and plates made of functionally graduated material, Brischetto [23] et Brischetto et al. [24], respectively. The calculated temperature profile gives an appropriate thermal load to properly study the thermal bending of these structures. In the works of the previous authors, the Fourier heat conduction equation was solved according to the technique presented by Tungikar et Rao [25].

II. Plate Formulation

A) Energy formulation

Consider a laminate composite thick plate of uniform thickness h , length a and width b , as shown on Fig. 1. The displacement of the plate are decomposed into three orthogonal components, u, v and w are the displacement components of middle plate in the x, y , and z directions, respectively. In accordance with the higher-order shear deformable theory [26], the displacements can be expressed as

$$\begin{aligned} u &= u_0 + z \theta_x - f(z) \left(\frac{\partial w_0}{\partial x} + \theta_x \right) \\ v &= v_0 + z \theta_y - f(z) \left(\frac{\partial w_0}{\partial y} + \theta_y \right) \\ w &= w_0 \end{aligned} \quad (1)$$

in which

$$f(z) = \frac{4}{3h^2} z^3 \quad (2)$$

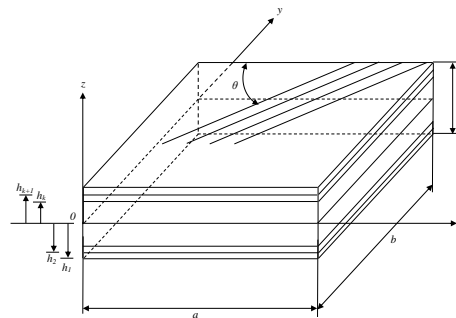


Figure 1. Laminate geometry with positive set of laminate reference axes, displacements and fiber orientation.

Where u_0, v_0 , and w_0 are the displacements of the middle surface of the plate, θ_x and θ_y are rotations of transverse normal about y -axis and x -axis of the plate respectively.

The linear strain-displacement relationships is given by

$$\begin{Bmatrix} \epsilon_{xx} \\ \epsilon_{yy} \\ \gamma_{xz} \\ \gamma_{xy} \end{Bmatrix} = \begin{Bmatrix} \frac{\partial u_0}{\partial x} \\ \frac{\partial v_0}{\partial y} \\ \frac{\partial w_0}{\partial y} + \theta_y \\ \frac{\partial w_0}{\partial x} + \theta_x \\ \frac{\partial v_0}{\partial x} + \frac{\partial u_0}{\partial y} \end{Bmatrix} + z \begin{Bmatrix} \frac{\partial \theta_x}{\partial x} \\ \frac{\partial \theta_y}{\partial y} \\ 0 \\ 0 \\ \frac{\partial \theta_x}{\partial x} + \frac{\partial \theta_y}{\partial y} \end{Bmatrix} - \frac{\partial f(z)}{\partial z} \begin{Bmatrix} 0 \\ 0 \\ \frac{\partial w_0}{\partial y} + \theta_y \\ \frac{\partial w_0}{\partial x} + \theta_x \\ 0 \end{Bmatrix} - f(z) \begin{Bmatrix} \frac{\partial^2 w_0}{\partial x^2} + \frac{\partial \theta_x}{\partial x} \\ \frac{\partial^2 w_0}{\partial y^2} + \frac{\partial \theta_y}{\partial y} \\ 0 \\ 0 \\ \frac{\partial \theta_x}{\partial x} + \frac{\partial \theta_y}{\partial y} + 2 \frac{\partial^2 w_0}{\partial x \partial y} \end{Bmatrix} \quad (3)$$

The constitutive equations for a k th layer, in the orthotropic local coordinate derived from Hook's law for plane stress is given by

$$\{\sigma\}^k = [C]^k \{\varepsilon\}^k \quad (4)$$

In the case of plane stress the stress vector can be written as

$$\{\sigma\}^k = \{\sigma_{xx} \quad \sigma_{yy} \quad \tau_{yz} \quad \tau_{xz} \quad \tau_{xy}\}^k \quad (5)$$

The constitutive equations for a k th layer, in the orthotropic local coordinate derived from Hook's law for plane stress are given by

$$\begin{Bmatrix} \sigma_1 \\ \sigma_2 \\ \sigma_{12} \\ \sigma_{13} \\ \sigma_{23} \end{Bmatrix}^k = \begin{bmatrix} C_{11} & C_{12} & 0 & 0 & 0 \\ C_{12} & C_{22} & 0 & 0 & 0 \\ 0 & 0 & C_{33} & 0 & 0 \\ 0 & 0 & 0 & C_{44} & 0 \\ 0 & 0 & 0 & 0 & C_{55} \end{bmatrix}^k \begin{Bmatrix} \varepsilon_1 \\ \varepsilon_2 \\ \varepsilon_{23} \\ \varepsilon_{13} \\ \varepsilon_{23} \end{Bmatrix}^k \quad (6)$$

Where the well-known engineering constants C_{ij} are given by

$$\begin{aligned} C_{11} &= E_1 / (1 - \nu_{1,2} \nu_{2,1}) & C_{22} &= E_2 / (1 - \nu_{1,2} \nu_{2,1}) & C_{12} &= \nu_{2,1} E_{12} / (1 - \nu_{1,2} \nu_{2,1}) \\ C_{21} &= C_{2,1} & C_{33} &= G_{1,2} & C_{44} &= G_{1,3} & C_{55} &= G_{2,3} \end{aligned} \quad (7)$$

In which E_i , ν_{ij} and G_{ij} are the Young's modulus, Poisson's ratio and shear modulus of the lamina. Where, 1 and 2 represent the directions parallel and perpendicular to the fibers direction. By performing a proper coordinate transformation, the stress-strain relationships of a single lamina in the $oxyz$ co-ordinate system can be obtained.

The stress-strain relations in the global (x, y, z) coordinate system can be written as

$$\begin{Bmatrix} \sigma_x \\ \sigma_y \\ \sigma_{xy} \\ \sigma_{xz} \\ \sigma_{yz} \end{Bmatrix}^k = \begin{bmatrix} Q_{11} & Q_{12} & Q_{13} & 0 & 0 \\ Q_{12} & Q_{22} & Q_{23} & 0 & 0 \\ Q_{13} & Q_{23} & Q_{33} & 0 & 0 \\ 0 & 0 & 0 & Q_{44} & Q_{45} \\ 0 & 0 & 0 & Q_{45} & Q_{55} \end{bmatrix}^k \begin{Bmatrix} \varepsilon_x \\ \varepsilon_y \\ \gamma_{xy} \\ \gamma_{xz} \\ \gamma_{yz} \end{Bmatrix}^k \quad (8)$$

The kinetic energy of a vibrating composite thick plate is given by

$$Ec = \frac{1}{2} \int_0^1 \int_0^1 [\dot{u}_0^2 + \dot{v}_0^2 + \dot{w}_0^2] dx dy \quad (9)$$

Where ρ is the mass density per unit volume.

The strain energy of a thick plate is expressed as

$$Ed = \frac{1}{2} \int_0^1 \int_0^1 [\sigma_x^k \varepsilon_x^k + \sigma_y^k \varepsilon_y^k + \sigma_{xy}^k \gamma_{xy}^k + \sigma_{xz}^k \gamma_{xz}^k + \sigma_{yz}^k \gamma_{yz}^k] dx dy \quad (10)$$

The thermoelastic vector for are obtained by

$$Ed_T = \frac{-1}{2} \iiint (\sigma_x \varepsilon_{T,xx} + \sigma_y \varepsilon_{T,yy} + \sigma_{xy} \gamma_{T,xy} + \sigma_{xz} \gamma_{T,xz} + \sigma_{yz} \gamma_{T,yz}) dx dy dz \quad (11)$$

ε_T represents the deformations due to the temperature gradient

$$\{\varepsilon_T\} = \begin{Bmatrix} \varepsilon_{T_{xx}} \\ \varepsilon_{T_{yy}} \\ \gamma_{T_{xy}} \\ \gamma_{T_{xz}} \\ \gamma_{T_{yz}} \end{Bmatrix} = \begin{Bmatrix} \alpha_{xx} \Delta T \\ \alpha_{yy} \Delta T \\ \alpha_{xy} \Delta T \\ 0 \\ 0 \end{Bmatrix} \quad (12)$$

With α_{xx} , α_{yy} et α_{xy} are the coefficients of thermal expansion.

B) Hierarchical finite element formulation

A four node rectangular hierarchical finite element with eight degrees of freedom per node ($u_0, v_0, w_0, \partial w_0/\partial x, \partial w_0/\partial y, \partial^2 w_0/\partial xy, \theta_x, \theta_y$) is developed on the basis of a third-order plate theory (See Fig. 2). Trigonometric hierarchical functions are used as shape functions. The model requires C^0 continuity for u_0, v_0, θ_x and θ_y and C^1 continuity for w_0 .

The displacements and rotations of the rectangular plate p-element are expressed as

$$\begin{aligned} u_0(\xi, \eta, t) &= \sum_{m=1}^{P_u} \sum_{n=1}^{P_u} q_{u_{mn}}(t) f_m(\xi) f_n(\eta) \\ v_0(\xi, \eta, t) &= \sum_{m=1}^{P_v} \sum_{n=1}^{P_v} q_{v_{mn}}(t) f_m(\xi) f_n(\eta) \\ w_0(\xi, \eta, t) &= \sum_{m=1}^{P_w} \sum_{n=1}^{P_w} q_{w_{mn}}(t) g_m(\xi) g_n(\eta) \\ \theta_x(\xi, \eta, t) &= \sum_{m=1}^{P_\theta} \sum_{n=1}^{P_\theta} q_{\theta_{x_{mn}}}(t) f_m(\xi) f_n(\eta) \\ \theta_y(\xi, \eta, t) &= \sum_{m=1}^{P_\theta} \sum_{n=1}^{P_\theta} q_{\theta_{y_{mn}}}(t) f_m(\xi) f_n(\eta) \end{aligned} \quad (11)$$

Where P_u, P_w and P_θ are the number of shape functions used in the model.

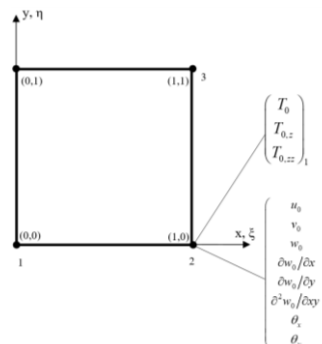


Figure 2. Plate element coordinates and dimensions

The first shape functions f_1, f_2 and g_1 to g_4 , are commonly used in the finite element method. The functions (f_{n+2} and g_{n+4}) are the trigonometric shape functions and lead to zero transverse displacement, and zero slope at each node. This feature is highly significant since these functions give additional freedom to the edges and the interior of the element.

The expressions of the trigonometric hierarchical shape functions $f_i(\xi)$ for C^0 continuity and $g_i(\xi)$ for C^1 are given by [27]

$$\begin{cases} f_1 = 1 - \xi \\ f_2 = \xi \\ f_{n+2} = \sin(\delta r \xi) \\ \delta r = r \pi \\ r = 1, 2, 3, \dots \end{cases} \quad (12)$$

and

$$\begin{cases} g_1 = 1 - 3\xi^2 + 2\xi^3 \\ g_2 = \xi - 2\xi^2 + \xi^3 \\ g_3 = 3\xi^2 - 2\xi^3 \\ g_4 = -\xi^2 + \xi^3 \\ g_{n+4} = \delta r \left[-\xi + (2 + (-1)^r) \xi^2 - (1 + (-1)^r) \xi^3 \right] + \sin(\delta r \xi) \\ \delta r = r \pi \\ r = 1, 2, 3, \dots \end{cases} \quad (13)$$

Where $\xi (= x/a)$ et $\eta (= y/b)$

The displacements and rotations can be expressed in matrix form as

$$\begin{Bmatrix} u_0 \\ v_0 \\ w_0 \\ \theta_x \\ \theta_y \end{Bmatrix} = [N] \{q\} \quad (14)$$

[N] is the matrix of shape functions, given by

$$[N] = \begin{bmatrix} [N_u] & 0 & 0 & 0 & 0 \\ 0 & [N_v] & 0 & 0 & 0 \\ 0 & 0 & [N_w] & 0 & 0 \\ 0 & 0 & 0 & [N_{\theta_x}] & 0 \\ 0 & 0 & 0 & 0 & [N_{\theta_y}] \end{bmatrix} \quad (15)$$

where

$$\{q\} = \begin{Bmatrix} q_u \\ q_v \\ q_w \\ q_{\theta_x} \\ q_{\theta_y} \end{Bmatrix} \quad (16)$$

In which $q_u, q_v, q_w, q_{\theta_x}$, and q_{θ_y} are the generalized displacements.

The matrices of shape functions are given by

$$[N_w] = \left[(g_1(\xi) g_1(\eta))_1, (g_1(\xi) g_2(\eta))_2, \dots, (g_k(\xi) g_l(\eta))_r, \dots, (g_{P_w}(\xi) g_{P_w}(\eta))_{P_w} \right] \quad (17)$$

where $k=1, \dots, P_w$, $l=1, \dots, P_w$, and $r=j+(i-1)P_w$

and

$$[N_u] = [N_\theta] = \left[(f_1(\xi) f_1(\eta))_1, (f_1(\xi) f_2(\eta))_2, \dots, (f_i(\xi) f_j(\eta))_m, \dots, (f_{P_\theta}(\xi) f_{P_\theta}(\eta))_{P_\theta} \right] \quad (18)$$

where $i=1, \dots, P_\theta$, $j=1, \dots, P_\theta$, and $m=j+(i-1)P_\theta$.

The equations of motion in the case of forced vibration of composite plates can be expressed as

$$[M]\{\ddot{q}\} + [K]\{q\} = F(t) \quad (19)$$

Here [K] is called the stiffness matrix of the p-element, determined from the strain energy

$$[K] = \begin{bmatrix} [K_{uu}] & [K_{uv}] & [K_{uw}] & [K_{u\theta_x}] & [K_{u\theta_y}] \\ [K_{uv}]^T & [K_{vv}] & [K_{vw}] & [K_{v\theta_x}] & [K_{v\theta_y}] \\ [K_{uw}]^T & [K_{vw}] & [K_{ww}] & [K_{w\theta_x}] & [K_{w\theta_y}] \\ [K_{u\theta_x}]^T & [K_{v\theta_x}]^T & [K_{w\theta_x}]^T & [K_{\theta_x\theta_x}] & [K_{\theta_x\theta_y}] \\ [K_{u\theta_y}]^T & [K_{v\theta_y}]^T & [K_{w\theta_y}]^T & [K_{\theta_x\theta_y}] & [K_{\theta_y\theta_y}] \end{bmatrix} \quad (20)$$

and [M] is called the mass matrix of the p-element, given by the following relation

$$[M] = \begin{bmatrix} [M_{uu}] & 0 & [M_{uw}] & [M_{u\theta_x}] & 0 \\ 0 & [M_{vv}] & [M_{vw}] & 0 & [M_{v\theta_y}] \\ [M_{uw}]^T & [M_{vw}]^T & [M_{ww}] & [M_{w\theta_x}] & [M_{w\theta_y}] \\ [M_{u\theta_x}]^T & 0 & [M_{w\theta_x}]^T & [M_{\theta_x\theta_x}] & 0 \\ 0 & [M_{v\theta_y}]^T & [M_{w\theta_y}]^T & 0 & [M_{\theta_y\theta_y}] \end{bmatrix} \quad (21)$$

C) Thermal formulation

Thermal analysis of stratified composite plate is modeled by a hierarchical finite element with four nodes and four sides (Fig. 2). this element has three degrees of freedom per node (T_0 , $T_{0,z}$, $T_{0,zz}$), respectively, temperature, gradient and curvature.

The temperatures in the (x, y) plane, is expressed using shape functions are given by the relations (12) The expression of the temperature in the (x, y) plane by the shape functions is given by the following relation:

$$T_0(\xi, \eta) = \sum_{i=1}^{M+2N+2} \sum_{j=1}^{M+2N+2} \varphi_{0(i,j)} f_i(x) f_j(y) = [N] \varphi \quad (22)$$

Where

$$[N] = \left[(f_1(\xi) f_1(\eta))_1, (f_1(\xi) f_2(\eta))_2, \dots, (f_i(\xi) f_j(\eta))_m, \dots, (f_{(M+2)}(\xi) f_{(N+2)}(\eta))_{(M+2)(N+2)} \right] \quad (23)$$

In the case of a stationary regime, the thermal study is governed by the following differential equation

$$CT + (A_1 + A_2)T = Ch \quad (24)$$

Where the conduction matrix is given by

$$A_1 = \int_0^1 \int_0^1 [B]^T [\bar{K}] [B] d\xi d\eta \quad (25)$$

And convection matrix given by

$$A_2 = hc \int_0^1 \int_0^1 [B]^T [R]^T [R] [B] d\xi d\eta \quad (26)$$

The capacitance matrix are obtained by

$$C = \int_0^1 \int_0^1 [B]^T [\bar{R}] [B] d\xi d\eta \quad (27)$$

The convection vector represents the external thermal loads in the form of convection

$$\{Q_c\} = hc \int_S [B]^T [\bar{R}]^T T_\infty ds \Big|_{(z=h_1, h_N)} \quad (28)$$

With

T_∞ : Surface temperature.

hc : convection imposed on the surface.

Vector external heat source are obtained by

$$\{Q_q\} = hc \int_S [B]^T [\bar{R}]^T q ds \Big|_{(z=h_1, h_N)} \quad (29)$$

The temperature on the walls is given by the following relation

$$\{Q_B\} = [A1] \{T\} \Big|_{(z=h_1, h_N)} \quad (30)$$

III. Numerical results and discussion

A) Dynamic study

In this section, solution accuracy and convergence studies of the present formulation are carried out. The convergence study is performed on [45/-45] angle-ply square plate with totally clamped (CCCC) edges and combined boundary condition. Figures 3 and 4 show that good convergence and accuracy of the first five frequency parameters are obtained by increasing the number of shape functions. The plate is considered as one element and the number of hierarchical terms is increased to 14 trigonometric functions in the case of EFFF plate, and 14 trigonometric functions for CCCC plate.

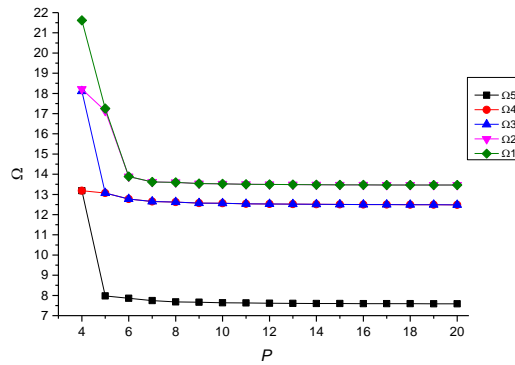


Figure 3. Convergence of frequency parameters $\Omega = \omega b^2/h \sqrt{\rho/E_2}p$ for totally clamped CCCC composite square plate ($a/h=2$).

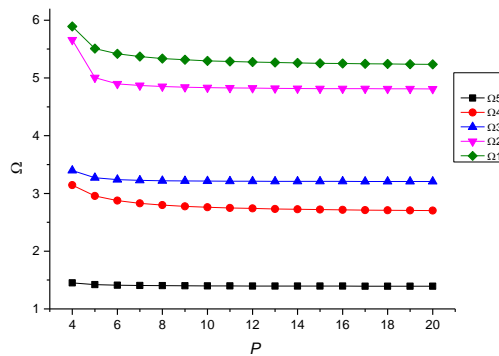


Figure 4. Convergence of frequency parameters $\Omega = \omega b^2/h \sqrt{\rho/E_2}p$ for CFFF composite square plate ($a/h=2$).

The effect of side-to-thickness ratio (a/h) on the vibration behavior of an antisymmetric $[0/90/\text{core}/0/90]$ sandwich square plate with simply supported edges are studied here. The material properties used in the present analysis are:

Facet sheets (Graphite-Epoxy T300/934)

$$E_1 = 131 \text{ Gpa}, E_2 = 10.34 \text{ Gpa}, G_{12} = 6.895 \text{ Gpa}, G_{13} = 6.205 \text{ Gpa}, G_{23} = 6.895 \text{ Gpa}, \nu_{12} = 0.22, \nu_{13} = 0.22, \nu_{23} = 0.49, \rho = 1627 \text{ kg/m}^3$$

Core properties (isotropic)

$$E_1 = E_2 = 6.89 \times 10^{-3} \text{ Gpa}, G_{12} = G_{13} = G_{23} = 3.45 \times 10^{-3} \text{ Gpa}, \nu_{12} = \nu_{13} = \nu_{23} = 0, \rho = 97 \text{ kg/m}^3$$

The results obtained for the fundamental frequency parameters as function of different side-to-thickness ratio (a/h) are given in Table 1. The results clearly show that the frequency values predicted by the present study are in good agreement with those of Reddy [28], Senthilnathan et al. [29], and those of Kant and Swaminathan [30] in which the displacements are expanded as cubic functions of the thickness coordinate. It is clear that the values given by FSDT [31] are higher than those predicted by HSDT models.

Table 1. Comparison of fundamental frequency parameters $\Omega = \omega(a^2/h) (\sqrt{\rho_c/E_{2c}})$ for SSSS of an antisymmetric $[0/90/\text{core}/0/90]$, sandwich plate with $a/b = 1$ and $hc/hf = 10$.

| a/h | Present | HSDT [28] | HSDT [29] | HSDT ^a [30] | HSDT ^b [30] | FSDT[31] |
|-----|---------|-----------|-----------|------------------------|------------------------|----------|
| 2 | 1.6260 | 1.6252 | 1.6252 | 1.1941 | 1.1734 | 5.2017 |
| 4 | 3.1039 | 3.1013 | 3.1013 | 2.1036 | 2.0913 | 9.0312 |
| 10 | 7.0529 | 7.0473 | 7.0473 | 4.8594 | 4.8519 | 13.8694 |
| 20 | 11.2725 | 11.2664 | 11.2664 | 8.5955 | 8.5838 | 15.5295 |
| 30 | 13.3723 | 13.6640 | 13.6640 | 11.0981 | 11.0788 | 15.9155 |
| 40 | 14.4440 | 14.4390 | 14.4390 | 12.6821 | 12.6555 | 16.0577 |
| 50 | 15.0366 | 15.0323 | 15.0323 | 13.6899 | 13.6577 | 16.1264 |
| 60 | 15.3911 | 15.3868 | 15.3868 | 14.3497 | 14.3133 | 16.1612 |
| 70 | 15.6174 | 15.6134 | 15.6134 | 14.7977 | 14.7583 | 16.1845 |
| 80 | 15.7699 | 15.7660 | 15.7660 | 15.1119 | 15.0702 | 16.1991 |
| 90 | 15.8770 | 15.8724 | 15.8724 | 15.3380 | 15.2946 | 16.2077 |
| 100 | 15.9551 | 15.9522 | 15.9522 | 15.5093 | 15.4647 | 16.2175 |

a: Model with 12 dofs, b: Model with 9 dofs

B) Thermal study

We consider the case of a square sandwich plate, consisting of five layers. The skin is made of aluminum and plastic reinforced with CFRP carbon fibers. The soul is also made of aluminum. The properties and thicknesses of the different layers are given in Table 2. Temperature flow on the upper part of the plate and a convection on the lower part. Figure 5 shows the points of the temperatures taken for a comparison. between the developed program and the FEM software following the z direction.

Table 2 : Thermal conduction and layer thickness of the sandwich plate.

| Layer | Thickness [m] | Materials | K_{xx} [W/m k] | K_{yy} [W/m k] | K_{zz} [W/m k] |
|-------|---------------|------------------------------|------------------|------------------|------------------|
| 1 | 0.03 | Aluminium | 235.0 | 235.0 | 235.0 |
| 2 | 0.05 | CFRP $[0^\circ, 90^\circ]$ s | 26.208 | 0.96 | 0.96 |
| 3 | 0.15 | Aluminium | 235.0 | 235.0 | 235.0 |
| 4 | 0.05 | CFRP $[0^\circ, 90^\circ]$ s | 26.208 | 0.96 | 0.96 |
| 5 | 0.03 | Aluminium | 235.0 | 235.0 | 235.0 |

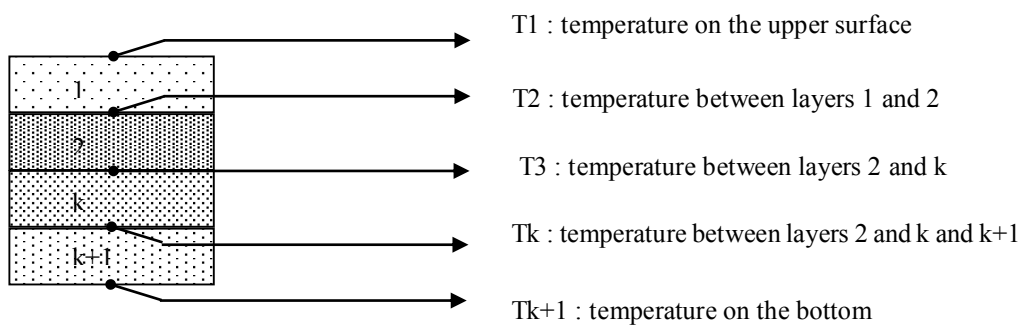


Figure 5. Temperatures used for comparison in the vertical direction of the Laminate layer ($k+1=NC$)

Table 3 shows the comparison of the results obtained by the present method with the results obtained by the FEM software, where it uses a cubic element with eight degrees of freedom. Note that the results obtained are identical with those of the FEM software.

In this part we made a comparison between two methods used to solve transient thermal problems. The present method PTIM (precise time integration method), the second the method of (finite differences) and the ANSYS software in order to validate the program. The thermal properties and geometric dimensions of the square plate used in this example are shown in Table 4.

Table 3. variation of the temperature in a five-layer sandwich plate with with $q_1 = 800 \text{ W/m}^2 \text{ K}$ et une

$$hc_2 = 40 \text{ W/m}^2 \text{ K} \text{ and } T_{\infty_2} = 5 \text{ C}^\circ .$$

| Temperature | present MEF P | FEM software |
|-------------|--------------------|--------------|
| T1 | 109.05 | 109.05 |
| T2 | 108.95 | 108.95 |
| T3 | 67.28 | 67.28 |
| T4 | 66.77 | 66.77 |
| T4 | 25.1 | 25.1 |
| T5 | 25 | 25 |

Table 4. Thermal conduction and thickness of the layers of the sandwich plate in the case of a transient thermal.

| Layer | Thickness [m] | | | Materials | | |
|----------------|------------------|------------------|------------------|-----------------|--------------|--|
| 1 | 0.03 | | | Aluminium | | |
| 2 | 0.05 | | | T300/934 | | |
| 3 | 0.15 | | | Aluminium | | |
| 4 | 0.05 | | | T300/934 | | |
| 5 | 0.03 | | | Aluminium | | |
| Materials | $K_{xx} [W/m k]$ | $K_{yy} [W/m k]$ | $K_{zz} [W/m k]$ | $\rho [kg/m^3]$ | $C [J/kg K]$ | |
| T300/934 | 5.73 | 5.73 | 5.73 | 1460 | 1300 | |
| Aluminium 6061 | 167.0 | 167.0 | 167.0 | 2700 | 896 | |

Figure 6 shows that the plotted curves are totally confounded, which shows the accuracy of the results obtained using the PTIM method.

C) Thermoelastic analysis

In this example we study the case of a sandwich plate consisting of five symmetrical layers [0/90/core/90/0]. The core is aluminum 5052 in the form of honeycomb and CFRP skin (Figure 7). The properties of both materials are shown in Table 5. The plate is subjected to a variable thermal flow on the upper part, given in table 8.28 and a convection on the lower part. the influence of thermal loading on the displacements of the plate are studied.

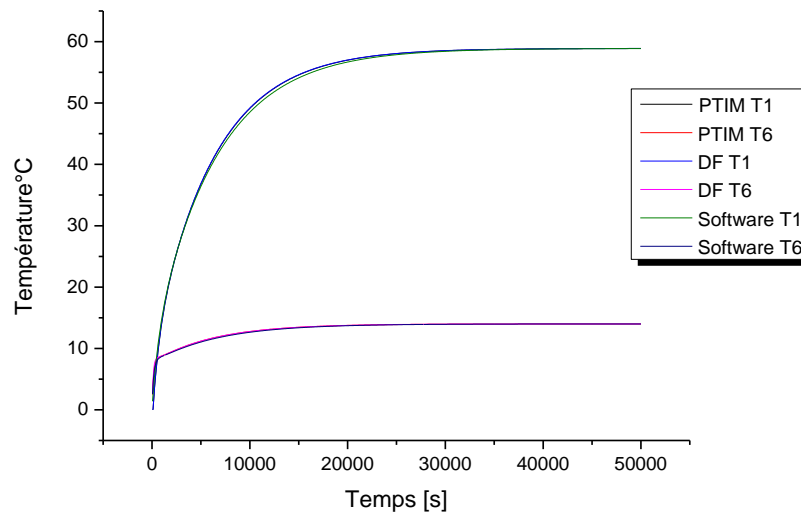


Figure 6. Variation of the temperature as a function of time in a sandwich plate.

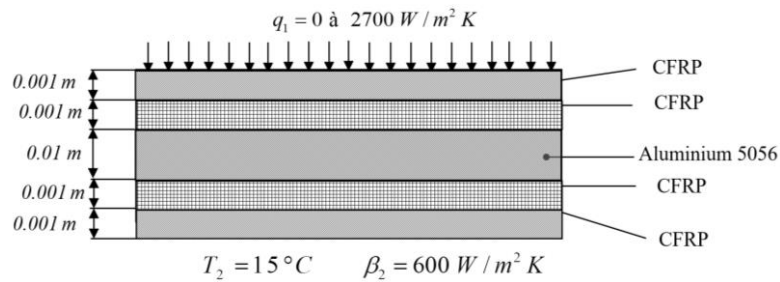


Figure 7: Sandwich plate, CFRP/Aluminum 5056.

Table 5. Properties of different materials of the sandwich plate

| Materials | Mechanical and thermo-mechanical properties | | | | | | |
|-------------------|---|---------------------|----------------|--------------------------|---------------------------------|-------|------------------------------------|
| | $k_{xx}/k_{yy}/k_{zz}$ ($W/m^2 K$) | ρ (kg/m^3) | C (J/kg C°) | E_{11}/E_{22} (GPa) | $G_{12}/G_{13}/G_{23}$ (GPa) | ν | α (C^{-1}) 10^{-6} |
| Aluminium 5052 | 2.1 | 48 | 921 | 0.41/0.24 | 0.15 | 0.3 | 23.76 |
| CFRP | 26.21/0.96/ 0.96 | 1600 | 1300 | 105/8.74 | 4.56 | 0.327 | 2.15 |

Size of the plate $a=1m, b=1m$

boundary condition q_1 varie de 0 à 2700 $W/m^2 K$; $\beta_2 = 600 W/m^2 K$; $T_{\infty 2}=15^\circ C$

Initial temperature $T_{init}=10^\circ C$

Table 6 shows the variation of heat flux applied to the plate

Figure 8 shows the variation of temperature T1 and T6 of the sandwich plate and Figure 9 shows the variation of the temperature gradient.

Table 6. heat flux variation as a function of time

| | | | | | | | | | |
|-----------------|---|-------|-----|--------|------|--------|------|--------|---------|
| q (W/m^2) | 0 | 337.5 | 675 | 1012.5 | 1350 | 1687.5 | 2025 | 2362.5 | 2700 |
| K) | | | | | | | | | |
| Time [s] | 0 | 0.5 | 1 | 1.5 | 2 | 2.5 | 3 | 3.5 | 4 à 800 |

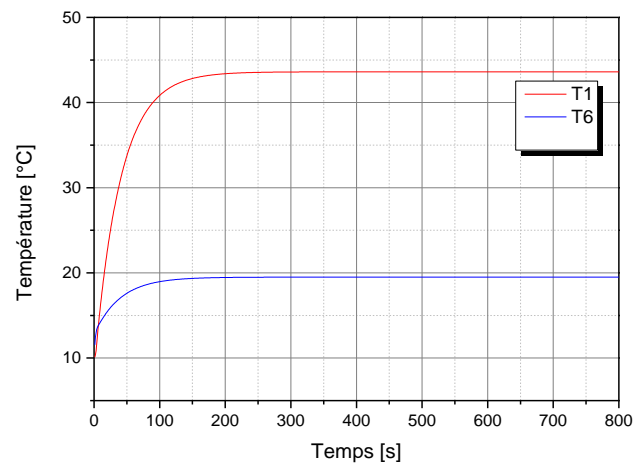


Figure 8. Variation of temperatures T1 and T6 as a function of time.

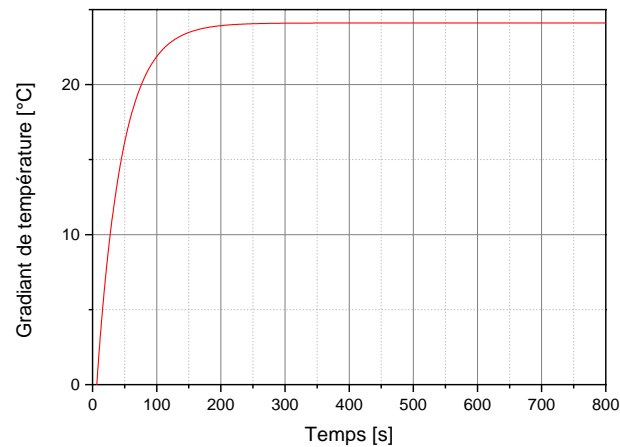


Figure 9. Variation of temperature gradient ΔT as a function of time.

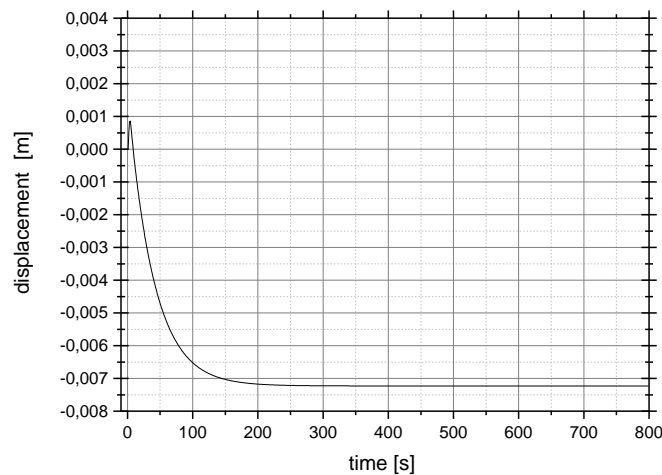


Figure 10. Representation of displacements under the effect of thermal loading as a function of time in the case of an E-L-L-L sandwich plate ($\xi = 1$, $\eta = 0.5$).

Figure 10 shows the variation in plate displacement as a function of time with varying heat flux loading from 0 to 2700 ($\text{W} / \text{m}^2 \text{K}$) in 4 seconds (Table 6). The influence of the temperature gradient is noted where the displacements follow the course of the temperature gradient, where the displacements decrease and stabilize in the stationary part.

IV. Conclusion

A new C1 HSDT p-element with eight degrees of freedom per node has been developed and used to find natural frequencies of laminated composite and sandwich thick plates in conjunction with Reddy's HSDT. It is well known that the plate theory is quite attractive but it could not be exploited as expected in finite element. This is due to the difficulties associated with C1 inter-element continuity discretized into one element and the number of trigonometric shape functions is varied. The p-element has been implemented with a very simple and understandable mathematical framework and is easily programmed. Monotonic and uniform convergence is found to occur as the number of trigonometric shape functions is increased. High accuracy, stable numerical computation, and rapid convergence have been observed in the analysis. The solutions of this model are found to be in excellent agreement with 3D elasticity solutions, analytical HSDT solutions, and the solutions from finite element models based on refined theories and Reddy's HSDT. Based on these observations, the element can be recommended for free vibration analysis of composite plate structures with sufficient accuracy.

Thermal conduction is modeled by the TLT theory, three degrees of freedom per node are considered with functions of type C1 and hierarchical trigonometric forms. Thermoelastic analysis is solved by the Newmark method. The results obtained using our developed calculation code are validated with FEM calculation code, a very good agreement is observed. The influence of thermal loading on displacements is studied.

REFERENCES

- [1] Nelson RB, Lorch DR. A refined theory for laminated orthotropic plates. ASME, J Appl Mech 1974; 41: 177-183.
- [2] Lo KH, Christen RM, Wu EM. A higher order theory of plate deformation – Part 1: Homogeneous plates. ASME, J Appl Mech 1979; 44: 663-668.
- [3] Nayak AK, Moy SSJ, Sheno RA. Free vibration analysis of composite sandwich plates based on Reddy's higher order theory. Composites Part B: Engineering 2002; 33 (7): 505-519.
- [4] Nayak AK, Sheno RA, Moy SSJ. Transient response of composite sandwich plates. Comput Struct 2004; 64: 249-267.
- [5] Batra RC, Aimmanee S. Vibrations of thick isotropic plates with higher order shear and normal deformable plate theories. Comput Struct 2005; 83: 934-955.
- [6] Ambartsumian SA. On the Theory of Bending Plates. Izv Otd Tech Nauk. AN SSSR 1958; 5:69–77.
- [7] Soldatos KP, Timarci T. A unified formulation of laminated composites, shear deformable, five-degrees-of-freedom cylindrical shell theories. Compos Struct 1993; 25: 165–171.
- [8] Reddy JN. Energy and variational methods in applied mechanics. Wiley, London 1984.
- [9] Padovan J. Steady conduction of heat in linear and nonlinear fully anisotropic media by finite elements. Journal of Heat Transfer 1974;96:313-8.
- [10] Tamma KK, Yurko AA. A unified finite element modelling/analysis approach for thermal structural response in layered composites. Computers & Structures 1988;29:743-54.
- [11] Bose A, Surana KS. Piecewise hierarchical p-version axisymmetric shell element for non-linear heat conduction in laminated composites. Computers & Structures 1993;47:1-18.
- [12] R. Rolfes, K. Rohwer, Integrated thermal and mechanical analysis of composite plates and shells, Composites Science and Technology 2000; 60 2097-2106
- [13] Heemskerk JF, Delil AAM, Daniels DHW. Thermal conductivity of honeycomb sandwich panels for space application. Technical report, National Aerospace Laboratory NLR, The Netherlands, 1971.
- [14] J. Noack, R. Rolfes, J. Tessler, New layer wise theories and finite elements for efficient thermal analysis of hybrid structures, Computers and Structures 2003; 81, 2525–2538.
- [15] Brischetto, S, Effect of the through-the-thickness temperature distribution on the response of layered and composite shells. International Journal of Applied Mechanics 2009; 1 (4), 1–25.
- [16] Brischetto S, Carrera E, Thermal stress analysis by refined multilayered composite shell theories. Journal of Thermal Stresses 2009; 32 (1), 165–186.
- [17] Khare, R.K, Kant, T, Garg, A.K. Closed-form thermo-mechanical solutions of higher-order theories of cross-ply laminated shallow shells. Composite Structures 2003; 59 (3), 313–340.
- [18] Khdeir, A.A. Thermoelastic analysis of cross-ply laminated circular cylindrical shells. International Journal of Solids and Structures 1996; 33 (27), 4007–4017.
- [19] Birsan, M. Thermal stresses in cylindrical Cosserat elastic shells. European Journal of Mechanics - A/Solids 2009; 28 (1), 94–101.
- [20] Carrera, E., An assessment of mixed and classical theories for the thermal stress analysis of orthotropic multilayered plates. Journal of Thermal Stresses 23 (9), 797–831.
- [21] Carrera, E., (2002). Temperature profile influence on layered plates response considering classical and advanced theories. AIAA Journal 2000; 40 (9), 1885–1896.
- [22] Rolfes, R., Noack, J., Taeschner, M. High performance 3D-analysis of thermo-mechanically loaded composite structures. Composite Structures 1999;46 (4), 367–379.
- [23] Brischetto, S. Effect of the through-the-thickness temperature distribution on the response of layered and composite shells. International Journal of Applied Mechanics 2009;1 (4), 1–25.
- [24] Brischetto, S., Leetsch, R., Carrera, E., Wallmersperger, T., Kröplin, B. Thermomechanical bending of functionally graded plates. Journal of Thermal Stresses 2008; 31 (3), 286–308.
- [25] Tungikar V, Rao, B.K.M. Three dimensional exact solution of thermal stresses in rectangular composite laminates. Composite Structures 1994; 27 (4), 419–430.
- [26] Asadi E, Fariborz SJ, Free vibration of composite plates with mixed boundary conditions based on higher-order shear deformation theory. Arch Appl Mech 2012; 82, 755–766.
- [27] Houmat A. An alternative hierarchical finite element formulation applied to plate vibrations. J Sound Vib 1997; 206(2): 201-215.



- [28] Reddy JN. A simple higher-order theory for laminated composite plates. ASME, J Appl Mech 1984; 51, 745-752.
- [29] Senthilnalhan NR, Lim KH, Lee KH, Chow ST. Buckling of shear deformable plates. AIAA J 1987; 25(9), 1268-71
- [30] Kant T, Swaminathan K. Analytical solutions for free vibration of laminated composite and sandwich plates based on a higher-order refined theory. Composite structures 2001, 53, 73-85
- [31] Whitney JM, Pagano NJ. Shear deformation in heterogeneous anisotropic plates. ASME, J Appl Mech 1970; 37(4), 1031-1036.